

Assessment of the Impact of Pile Characteristics on the Horizontal Displacement of Retaining Walls under Heavy Rainfall: A Case Study in Vietnam

Phuong Tuan Nguyen

Mien Tay Construction University, Vinh Long Province, Vietnam
tuanphuongvk@gmail.com

Luan Nhat Vo

Faculty of Engineering and Technology, Van Hien University, Ho Chi Minh City, Vietnam
luanvn@vhu.edu.vn

Truong Xuan Dang

Ho Chi Minh University of Natural Resources and Environment, Ho Chi Minh City, Vietnam
dxtruong@hcmunre.edu.vn

Hoa Van Vu Tran

The SDCT Research Group, University of Transport Ho Chi Minh City, Ho Chi Minh City, Vietnam
hoa.tranvu.htgroup@gmail.com

Tuan Anh Nguyen

University of Transport Ho Chi Minh City, Ho Chi Minh City, Vietnam
tuanna@ut.edu.vn (corresponding author)

Received: 17 December 2024 | Revised: 24 January 2025 | Accepted: 2 February 2025

Licensed under a CC-BY 4.0 license | Copyright (c) by the authors | DOI: <https://doi.org/10.48084/etasr.9957>

ABSTRACT

This study evaluates how pile characteristics influence the Horizontal Displacement (U_x) of river retaining walls in Ho Chi Minh City, Vietnam, during heavy rainfall, which floods the walls, while the river water level remains at its lowest. The study utilizes Finite Element Method (FEM) in combination with statistical methods, such as linear regression and Pearson correlation, to examine the effects of pile factors. These factors are the Number of Piles (NoP), Pile Spacing (PS), Pile Diameter (PD), and Pile Type (PT) based on the U_x of the river retaining walls. Finite element simulations are conducted across different scenarios to evaluate the impact of the aforementioned factors under dynamic environmental conditions. The study results show significant variation in the U_x of the retaining walls based on each factor. PS and PD have a strong influence on U_x , with correlation coefficients of 0.585 and -0.549, respectively. This indicates that a larger PS increases displacement, while a smaller PD also leads to greater displacement. In contrast, NoP has a weak correlation with U_x . The linear regression models suggest that these factors do not have an equal impact on the retaining wall stability. It is concluded that optimizing the pile characteristics, particularly PS and PD, can help minimize U_x . This enhances the stability of river retaining walls under harsh climatic conditions.

Keywords-pile characteristics; horizontal displacement; retaining walls; heavy rainfall; FEM

I. INTRODUCTION

The Saigon River retaining walls play a crucial role in protecting construction projects from erosion and the impact of

flowing water. This is especially essential in the context of Ho Chi Minh City, where there has been a significant increase in construction activities along the riverbanks. However, maintaining the stability of these retaining walls faces

numerous challenges, particularly under extreme climate conditions, such as heavy rainfalls, when the river water level is at its lowest. A heavy rainfall can cause flooding around the retaining wall, generating strong dynamic forces that affect its stability and cause U_x . This necessitates a thorough study of the retaining wall design methods, particularly under the rapidly changing geological and environmental conditions. The current research primarily focuses on analyzing the static factors that affect the stability of the retaining walls, such as the stress and load-bearing capacity of the wall structures [1-5]. However, the study of heavy rainfall and erosion due to low river water levels remains limited. Previous studies have mainly examined factors, such as the NoP, PS, and PT [6-9]. Nevertheless, few comprehensive studies have addressed the combined effects of these factors under the impact of extreme weather conditions, such as heavy rainfall that floods the wall and low river water levels.

II. MATERIALS AND METHODS

The study was conducted along the riverbank in Ho Chi Minh City, Vietnam, an area with complex geological characteristics, as shown in Figure 1. Its geology consists of four main layers: a 2-meter-thick filler, a 20-meter-thick muck layer, a 32-meter-thick clay layer, and a 70-meter-thick sand layer, as presented in Table I. The types of the selected piles are square and round piles with diameters of 350 mm, 400 mm, and 450 mm, as depicted in Table II. These pile sizes were chosen to investigate their impact on the U_x of river retaining walls. The retaining walls were designed with a thickness of 300 mm and a length of 2500 mm, supported by a foundation with a thickness of 400 mm and a length of 3000 mm, as portrayed in Table III. An applied load of 10 kN represents the operational load.

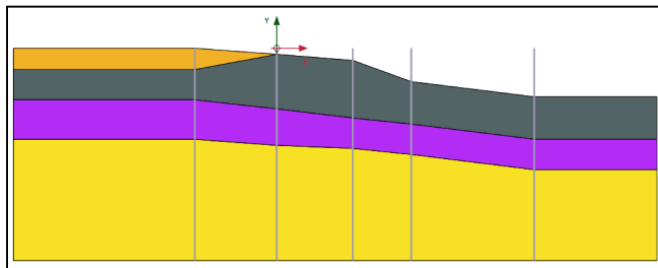


Fig. 1. Geological cross-section.

TABLE I. SOIL DESCRIPTION PARAMETERS

Hardening soil	Fill layer	Mud layer	Clay layer	Sand layer
Drainage type	Drained	Undrained	Undrained	Undrained
γ_{unsat} (kN/m ³)	18.6	14.2	18.1	20.1
γ_{sat} (kN/m ³)	19.4	15.1	18.2	20.3
e_{int}	0.62	1.81	0.72	0.61
P^{ref} (kN/m ²)	10^2	10^2	2×10^2	4×10^2
E_{50}^{ref} (kN/m ²)	8×10^3	4.6×10^3	24×10^3	36×10^3
E_{oed}^{ref} (kN/m ²)	8×10^3	4.6×10^3	24×10^3	36×10^3
E_{ur}^{ref} (kN/m ²)	24×10^3	13.8×10^3	72×10^3	108×10^3
ϕ (°)	26.6	18.5	23.5	30
c' (kN/m ²)	4.5	17.8	32	5.4

TABLE II. DESCRIPTION PARAMETERS OF THE PILE MATERIAL

Parameter	Square piles	Round piles
Material type	Elastic	Elastic
E (kN/m ²)	30×10^6	30×10^6
Y (kN/m ³)	10	10
Width (mm)	350; 400; 450	350; 400; 450
Thickness (mm)	-	80
Lspacing (mm)	500; 1000; 1500; 2000; 2500	500; 1000; 1500; 2000; 2500

TABLE III. DESCRIPTION PARAMETERS OF THE SOIL RETAINING WALL MATERIAL

Parameter	Foundations	Soil retaining wall
Material type	Elastic	Elastic
EA1 (kN/m)	12×10^6	9×10^6
EA2 (kN/m)	12×10^6	9×10^6
EI (kN m ² /m)	160×10^3	67.5×10^3
D (mm)	400	300
w (kN/m/m)	10	7.5
ν	0.2	0.2

The research methodology applies FEM using the PLAXIS 2D software. Figure 2 demonstrates the 15-noded elements, which simulate real-world conditions affecting the retaining wall system, particularly under heavy rainfall that floods the wall, while the river water level is at its lowest [10, 11].

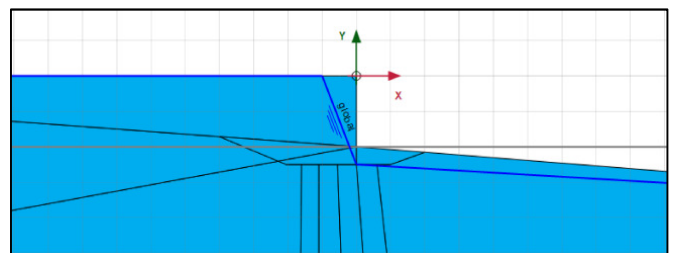


Fig. 2. Flow conditions.

The simulation scenarios include changes in PS, PD, PT, and NoP to study their effects on the U_x of the retaining wall. The simulations were carried out with three different NoP configurations: three piles, four piles, and five piles while varying PS from 500 mm to 2500 mm, as can be seen in Figures 3-5.

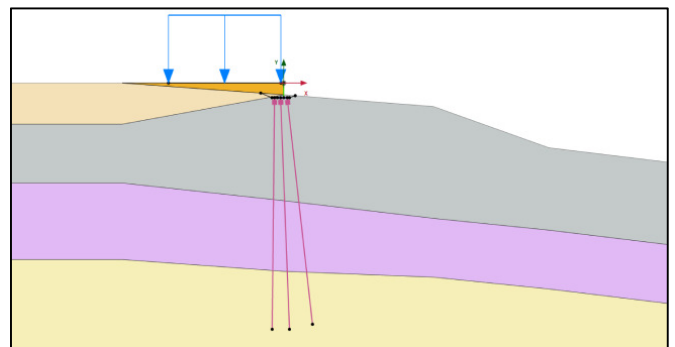


Fig. 3. The scenario with three piles.

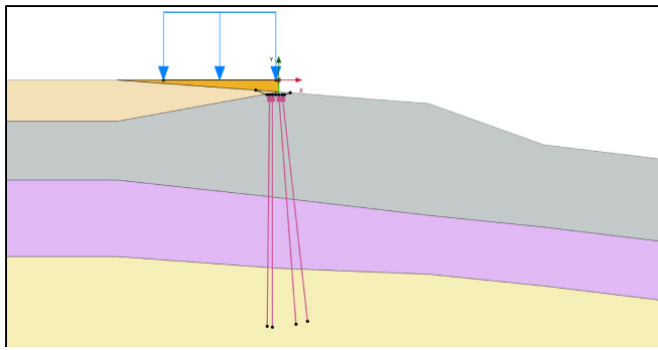


Fig. 4. The scenario with four piles.

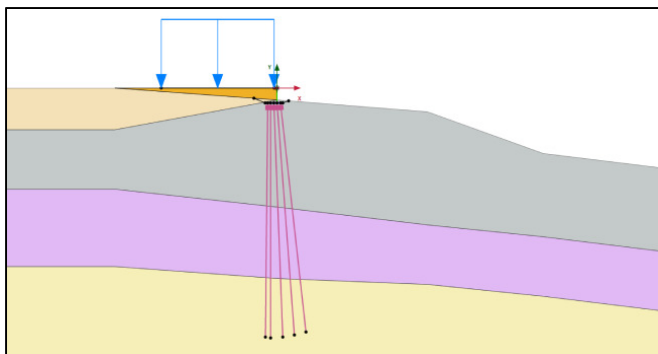


Fig. 5. The scenario with five piles.

The results from the FEM simulations are used as an input for the Pearson correlation analysis and linear regression to determine the relationship between the NoP, PS, PD, and PT factors with the U_x of the retaining wall. Statistical tests, such as ANOVA and R-squared, are used to assess the statistical significance of the results [12, 13]. To check for multicollinearity among the predictor variables, the Variance Inflation Factor (VIF) is applied, and the impact of these factors is determined through the Beta coefficient.

III. RESULTS

According to Figure 6 and Table IV, the FEM results across 80 scenarios affecting the U_x of the foundation system exhibit an average value of 128.1 mm. Figure 7 demonstrates that in the 5 square pile scenario, a PS of 500 mm, a PD of 350 mm, and a U_x of 104.5 mm were obtained. The Pearson correlation analysis examines the relationship between NoP, PS, PD, PT, and U_x , as outlined in Table V.

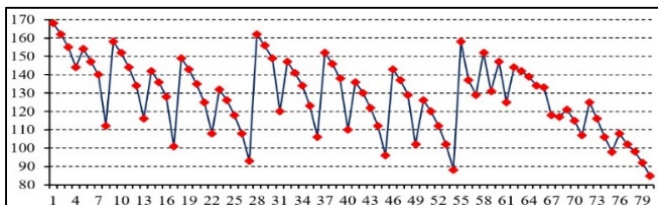


Fig. 6. U_x results.

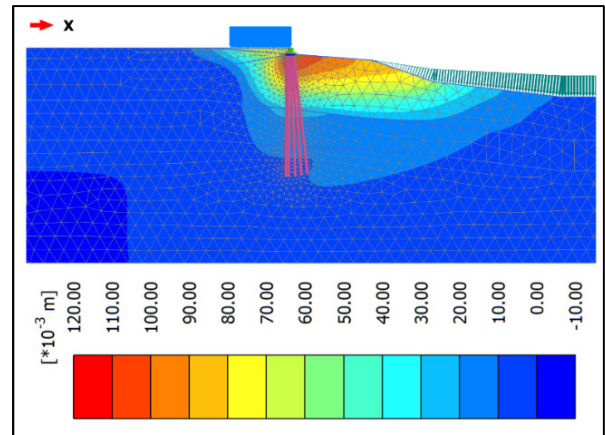


Fig. 7. Total displacements U_x (5 square piles, PS 500, PD 350).

TABLE IV. DESCRIPTIVE STATISTICS

Variables	Min	Max	Mean	Std. Deviation
NoP	3	5	3.99	0.819
PS	500	2500	1556.3	724.8
PD	350	450	401.9	40.9
PT	1	2	1.48	0.5
U_x	84.9	168	128.1	19.8

TABLE V. PEARSON CORRELATION

Variables	NoP	PS	PD	PT	U_x	
NoP	Pearson	1	-0.041	-0.018	-0.047	-0.252
	Sig.		0.715	0.873	0.679	0.024
PS	Pearson	-0.041	1	-0.025	0.065	0.585
	Sig.	0.715		0.826	0.568	0.000
PD	Pearson	-0.018	-0.025	1	-0.013	-0.549
	Sig.	0.873	0.826		0.908	0.000
PT	Pearson	-0.047	0.065	-0.013	1	0.463
	Sig.	0.679	0.568	0.908		0.000
U_x	Pearson	-0.252	0.585	-0.549	0.463	1
	Sig.	0.024	0.000	0.000	0.000	

The correlation coefficient between NoP and U_x is -0.252, with a significance value of 0.024, indicating a weak relationship. PS has a correlation coefficient of 0.585 and a significance level of 0, meaning that a larger PS results in greater displacement. On the other hand, PD has a negative correlation with U_x , with a correlation coefficient of -0.549 and a significance level of $0 < 0.05$, indicating that a larger diameter reduces U_x . PT has a moderate correlation with U_x , with a correlation coefficient of 0.463 and a significance level of 0, showing that different PTs significantly affect displacement. The relationship between the independent variables (NoP, PS, PD, and PT) is generally weak, as indicated by the low correlation coefficients. This analysis highlights that although PS and PD are important factors in influencing U_x , NoP, and PT also play significant roles, albeit to a lesser extent.

TABLE VI. ANOVA

Model	Sum of squares	df	Mean square	F	Sig.	
1	Regression	26298.753	4	6574.688	108.396	0.000b
	Residual	4549.075	75	60.654		
	Total	30847.829	79			

a. Dependent variable: U_x
 b. Predictors: (Constant), PT, PD, NoP, PS

Table VII displays an adjusted R² value of 0.853, indicating that the independent variables explain 85.3% of the variation in the dependent variable U_x.

TABLE VII. MODEL SUMMARY

Model	R	R ²	Adjusted R ²	Std. error of the estimate	Durbin-Watson
1	0.923 a	0.853	0.845	7.788090	1.368
a. Predictors: (Constant), PT, PD, NoP, PS					
b. Dependent Variable: U _x					

Table VIII shows that the significance value in the regression model is less than 0.05, confirming that the independent variables significantly impact the dependent variable. Additionally, the VIF coefficient is below 2, indicating no multicollinearity and ensuring unbiased regression estimates.

TABLE VIII. COEFFICIENTS

Variable	Unstandardized coefficients		Standardized beta coefficients	t	Sig.	Collinearity statistics	
	B	Std. error				Tolerance	VIF
Constant	206.446	10.356		19.935	0		
NoP	-5.325	1.072	-0.221	-4.967	0	0.996	1.00
PS	0.015	0.001	0.536	12.049	0	0.994	1.00
PD	-0.258	0.021	-0.534	-12.038	0	0.999	1.00
PT	16.152	1.749	0.411	9.234	0	0.994	1.00
a. Dependent variable: U _x							

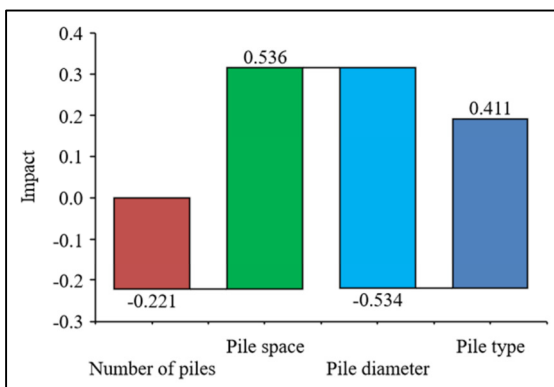


Fig. 8. The impact of independent variables on the dependent variable (U_x).

The negative sign indicates that the relationship between the factors is opposite to the increase of the U_x variable. The importance of the observed variables in affecting U_x, in descending order, is: PS, PD, PT, and NoP, as illustrated in Figure 8.

As evidenced in Table IX, the residual value ϵ is 7.588. A histogram of normalized residuals and a Normal P-P plot are used to check this value. As can be seen in Figure 9, the residual value columns have a bell-shaped curve, confirming that the distribution is approximately normal, and the assumption of normal distribution of residuals is not violated. The mean value is $-1.23E^{-15}$, close to 0, and the standard deviation of 0.974, is close to 1.

TABLE IX. RESIDUAL STATISTICS

Variable	Minimum	Maximum	Mean	Std. deviation
Predicted Value	87.18865	169.01671	128.10375	18.245427
Residual	14.464009	28.861284	0.000000	7.588362
Std. Predicted Value	-2.242	2.242	0.000	1.000
Std. Residual	-1.857	3.706	0.000	0.974
a. Dependent Variable: U _x				

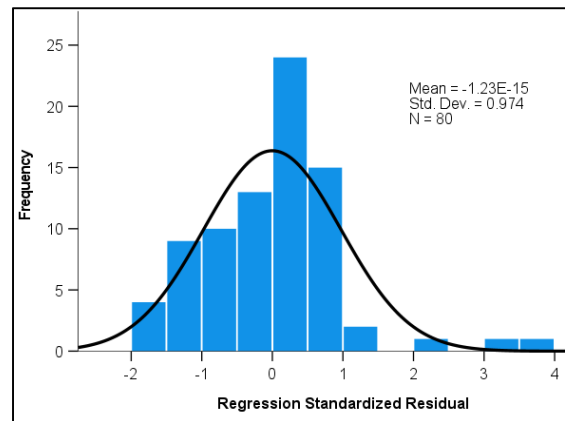


Fig. 9. Histogram of normalized residuals (U_x).

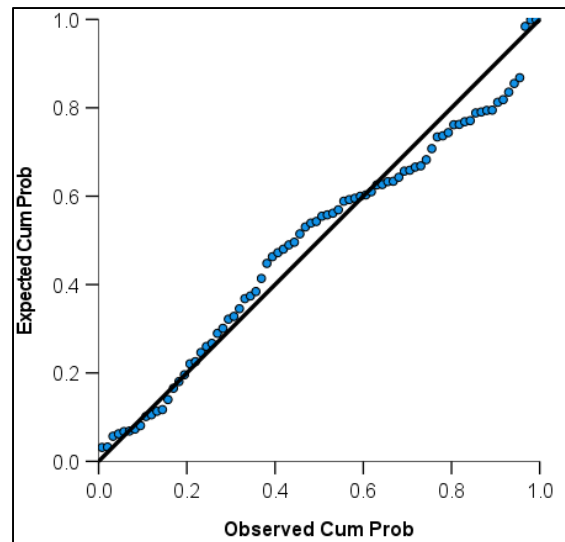


Fig. 10. Normal P-P Plot of regression standardized residual.

The residual data points almost align with the diagonal line, indicating that the residuals are approximately normally distributed, as portrayed in Figure 10. Therefore, the assumption of normal distribution of residuals is not violated. However, Table X demonstrates that some points deviate significantly from the diagonal line, implying the presence of outliers.

TABLE X. OUTLIERS OF TARGET DISPLACEMENT (UX)

Scenarios	Displacement Ux (mm)	Cook's distance
55	158	0.32
56	137	0.196
66	133	0.081
62	144	0.07
31	120	0.062

Cook's distance and Ux values for different scenarios help identify significant data points in the regression study. Scenarios with high Cook's distance, such as 55 and 56, have a substantial impact on the model's predictions, suggesting that these observations may disproportionately influence the regression parameters. In contrast, scenarios with lower Cook's distance values have a minimal impact, making the findings more reliable and reflective of the overall trend. Based on the results and residual value tests, the predictive formula for Ux displacement is:

$$U_x = 214.034 - 5.325\text{NoP} + 0.015\text{PS} - 0.258\text{PD} + 16.152\text{PT}$$

The comparison between the predicted results from the regression model and the observed values during a heavy rainfall event showed minimal deviation. In a practical application involving four square piles, with a spacing of 1000 m and a diameter of 400 mm, the prediction accuracy closely matched the observed data.

IV. DISCUSSION

The study results exhibit that Ux varies significantly under the influence of factors, such as the NoP, PS, PD, and PT. The FEM simulations reveal that as the NoP increases, the Ux of the retaining wall decreases, with a correlation coefficient of -0.252 between NoP and Ux, indicating a weak but notable relationship. Meanwhile, PS has a stronger influence on Ux, with a correlation coefficient of 0.585 and a significance level of 0. This indicates that as the spacing between the piles increases, the retaining wall Ux also increases. The PD and PT also have significant impacts on Ux, particularly PD, with a correlation coefficient of -0.549, suggesting that larger diameter piles help reduce the retaining wall Ux. The Beta coefficients in the linear regression model indicate that these factors have uneven effects, with PS and PD having the strongest influence. It can be also observed that the results of the current work are consistent with those of former research, which has shown that increasing the NoP helps improve the retaining wall stability. However, other studies have suggested that a too large spacing between piles may cause uneven displacement, reducing the retaining wall's effectiveness. These results confirm that optimizing the pile characteristics is necessary to ensure long-term structure stability. Moreover, according to the present study's findings, the key factors influencing the Ux of the retaining wall are the NoP, PS, and PD. Both PS and PD have a significant impact on Ux, whereas PT has a moderate effect. To optimize the retaining wall stability, it is proposed to reduce the spacing between the piles and increase the pile depth.

V. CONCLUSIONS

This study evaluated the impact of pile characteristics on the Horizontal Displacement (Ux) of the Saigon River retaining walls in Ho Chi Minh City, Vietnam, under dynamic environmental and heavy rainfall conditions. The results exhibited that the Ux of the retaining wall is significantly influenced by factors, such as the Number of Piles (NoP), Pile Spacing (PS), Pile Diameter (PD), and Pile Type (PT). The Finite Element Method (FEM) simulations and regression analysis indicated that as the NoP increases, the retaining wall Ux decreases, although this relationship is weak. PS has a stronger impact, with Ux increasing as the spacing between the piles becomes larger. Particularly, PD strongly influences the stability of the retaining wall, as larger diameter piles help reduce the retaining wall Ux. These findings emphasize the need to optimize the pile factors to enhance the stability of river retaining structures. Moreover, during the design of the riverbank retaining walls, priority should be given in choosing the right number, spacing, and diameter of piles, considering the local geological conditions and the stability requirements of the structure. Potential improvements in the design include reducing the spacing between the piles and increasing PD to minimize Ux, thereby enhancing the retaining wall stability. The FEM model deployed in this study was primarily based on the specific conditions of the study area and did not account for long-term soil and environmental changes. Therefore, future research may focus on developing more flexible simulation models that better reflect changes in geological conditions and environmental factors. Additionally, the study could be expanded to areas with different geological characteristics or areas subjected to more extreme climatic conditions, hence increasing the practical applicability of the research.

REFERENCES

- [1] G. Santhoshkumar and P. Ghosh, "Seismic stability analysis of a hunchbacked retaining wall under passive state using method of stress characteristics," *Acta Geotechnica*, vol. 15, no. 10, pp. 2969–2982, Oct. 2020, <https://doi.org/10.1007/s11440-020-01003-w>.
- [2] A. R. Karkanaki, N. Ganjian, and F. Askari, "Stability Analysis and Design of Cantilever Retaining Walls with Regard to Possible Failure Mechanisms: An Upper Bound Limit Analysis Approach," *Geotechnical and Geological Engineering*, vol. 3, no. 35, pp. 1079–1092, Jan. 2017, <https://doi.org/10.1007/s10706-017-0164-5>.
- [3] H. A. Chehade, X. Guo, D. Dias, M. Sadek, O. Jenck, and F. H. Chehade, "Reliability analysis for internal seismic stability of geosynthetic-reinforced soil walls," *Geosynthetics International*, vol. 30, no. 3, pp. 296–314, Jun. 2023, <https://doi.org/10.1680/jgein.22.00250>.
- [4] A. GuhaRay and D. K. Baidya, "Reliability Coupled Sensitivity-Based Seismic Analysis of Gravity Retaining Wall Using Pseudostatic Approach," *Journal of Geotechnical and Geoenvironmental Engineering*, vol. 142, no. 6, Jun. 2016, Art. no. 04016010, [https://doi.org/10.1061/\(ASCE\)GT.1943-5606.0001467](https://doi.org/10.1061/(ASCE)GT.1943-5606.0001467).
- [5] V. Sundaravel and G. R. Dodagoudar, "Deformation and Stability Analyses of Hybrid Earth Retaining Structures," *International Journal of Geosynthetics and Ground Engineering*, vol. 6, no. 3, Aug. 2020, Art. no. 37, <https://doi.org/10.1007/s40891-020-00222-1>.
- [6] K. Papadopoulou and A. Sofianos, "Factors Affecting the Behaviour of Retaining Structures with Prestressed Anchorages Under 2D and 3D Conditions," *Geotechnical and Geological Engineering*, vol. 34, no. 6, pp. 1877–1887, Dec. 2016, <https://doi.org/10.1007/s10706-016-9997-6>.
- [7] S. M. Ahmed and B. M. Basha, "External Stability Analysis of Narrow Backfilled Gravity Retaining Walls," *Geotechnical and Geological*

- Engineering, vol. 39, no. 2, pp. 1603–1620, Feb. 2021, <https://doi.org/10.1007/s10706-020-01580-3>.
- [8] S. Nimbalkar, A. Pain, and V. S. R. Annareddy, "A Strain Dependent Approach for Seismic Stability Assessment of Rigid Retaining Wall," *Geotechnical and Geological Engineering*, vol. 38, no. 6, pp. 6041–6055, Dec. 2020, <https://doi.org/10.1007/s10706-020-01412-4>.
- [9] P. J. Fox, "Analytical Solutions for Internal Stability of a Geosynthetic-Reinforced Soil Retaining Wall at the Limit State," *Journal of Geotechnical and Geoenvironmental Engineering*, vol. 148, no. 10, Oct. 2022, Art. no. 04022076, [https://doi.org/10.1061/\(ASCE\)GT.1943-5606.0002844](https://doi.org/10.1061/(ASCE)GT.1943-5606.0002844).
- [10] A. R. Kalantari and A. Johari, "System Reliability Analysis for Seismic Stability of the Soldier Pile Wall Using the Conditional Random Finite-Element Method," *International Journal of Geomechanics*, vol. 22, no. 10, Oct. 2022, Art. no. 04022159, [https://doi.org/10.1061/\(ASCE\)GM.1943-5622.0002534](https://doi.org/10.1061/(ASCE)GM.1943-5622.0002534).
- [11] C.-C. Huang and Y.-H. Chen, "Seismic Stability of Soil Retaining Walls Situated on Slope," *Journal of Geotechnical and Geoenvironmental Engineering*, vol. 130, no. 1, pp. 45–57, Jan. 2004, [https://doi.org/10.1061/\(ASCE\)1090-0241\(2004\)130:1\(45\)](https://doi.org/10.1061/(ASCE)1090-0241(2004)130:1(45)).
- [12] L. N. Vo, T. X. Dang, P. T. Nguyen, H. V. V. Tran, and T. A. Nguyen, "A Novel Methodological Approach to assessing Deformation and Force in Barrette Walls using FEM and ANOVA," *Engineering, Technology & Applied Science Research*, vol. 14, no. 5, pp. 16395–16403, Oct. 2024, <https://doi.org/10.48084/etasr.7975>.
- [13] T. X. Dang, P. T. Nguyen, T. A. Nguyen, and H. V. V. Tran, "Optimization of Barrette Wall Depths for Urban Excavation Stability Using FEM and ANOVA Testing," *Civil Engineering and Architecture*, vol. 12, no. 5, pp. 3530–3544, Sep. 2024, <https://doi.org/10.13189/cea.2024.120529>.